Suplemento de la Revista Mexicana de Física **3** 0308022 (2022) 1–5

Photo- and hadron-production of mesons

Łukasz Bibrzycki

Institute of Computer Science, Pedagogical University of Krakow,
ul. Podchorażych 2, 30-084 Kraków, Poland
on behalf of the JPAC collaboration.

Received 16 January 2022; accepted 27 February 2022

We discuss the $\pi\eta^{(\prime)}$ production in the double Regge model. We also identify the dominant exchanges necessary to describe the $\pi\eta^{(\prime)}$ system for energies above the resonance region. The model explains the forward-backward asymmetry observed in this reaction by associating it with the exotic $P-$wave, which in turn is related to the production of the putative π_1 hybrid meson. We also discuss the $\pi^+\pi^-$ production through two complementary mechanisms - direct resonance production (with subsequent $\pi^+\pi^-$ decay) and the Deck mechanism. The interference of the Deck and direct production explains the di-pion mass distribution for invariant masses below 2 GeV. Model predictions are compatible with the $q\bar{q}$ nature of the lightest $P-$ and $D-$wave resonances, whereas they hint towards substantial molecular or tetraquark component of the $f_0(980)$.

Keywords: hadron spectroscopy; Regge exchange; photoproduction; resonances.

DOI: https://doi.org/10.31349/SuplRevMexFis.3.0308022

1. Introduction

The QCD is believed to be the true theory of strong nuclear interactions. However, its application outside the perturbative region, *e.g.* to describe the observable features of hadrons, like masses and decay widths as well as their production mechanisms, requires either resorting to lattice regularisation or employing the QCD inspired models. With the advent of hadron spectroscopy oriented experiments like COMPASS at CERN or CLAS12 and GlueX at Jefferson Lab the hadron community obtained a unique opportunity to test lattice and model predictions, especially that these experiments are able to accumulate data sets largely surpassing the amounts of data available so far. Accurate and theoretically constrained models are especially important for the description of the exotic states which are actively searched for in many experiments. Due to notorious computational difficulty of QCD in the energy range typical for hadronic processes the amplitudes are constructed so that they fulfill the theoretical constraints like relativistic invariance, unitarity, analyticity and crossing symmetry. Two kinds of hadron processes are particularly relevant for searches of exotic states. These are the photoproduction of a few meson systems and the hadroproduction of one particular system, namely the $\pi\eta$ (or $\pi\eta'$) pair. The suitability of photoproduction process as a testing ground for exotic meson searches was pointed out in [1]. The $\pi\eta^{(\prime)}$ production is interesting because all resonances emerging in odd $\pi\eta^{(\prime)}$ partial waves are exotic [2]. Here, we collect the main results obtained recently by the JPAC collaboration for these two processes.

We start from the description of the $\pi^- p \to \pi^-\eta p$ and $\pi^- p \to \pi^-\eta' p$ reactions studied recently by the COMPASS collaboration at CERN [3]. The experiment revealed the clear angular asymmetry in the production of pions and η mesons with additional enhancement of the effect in the case of η' meson. The asymmetry has been attributed to the interference of the even and odd partial waves, especially the $P-$wave which is the strongest odd wave in the $\pi\eta^{(\prime)}$ system. The prominence of the $P-$wave can be linked to the π_1 resonance production commonly interpreted as the hybrid. On the other hand, the asymmetry enhancement observed in $\pi\eta'$ production as compared to $\pi\eta$ hints towards the role of gluonic degrees of freedom due to substantial gluonic content of the η' meson.

Then, we move on to discuss the $\gamma p \to \pi^+\pi^- p$ reaction. The $\pi^+\pi^-$ system by itself is not exotic, still it has resonances in various partial waves whose production mechanisms are far from firmly established. Additionally, we were interested in the interplay of the $\pi\pi$ rescattering dynamics and the pion-nucleon scattering which involves the one pion exchange. To evaluate our model we used the data obtained by the CLAS collaboration [4].

2. $\pi\eta^{(\prime)}$ production in the double Regge limit

The multi-Regge exchange formalism was studied by several authors in the past and has been extensively reviewed by Brower, DeTar and Weis in [5]. Here, we essentially follow the formalism and notation from that paper. In spite of considerable theoretical activity in the field, the phenomenological status of multi-Regge exchange models has been scrutinized to much lesser extent. The intent of the work [6] by the JPAC collaboration was to fill this gap at least partially.

The $\pi^- p \to \pi^-\eta^{(\prime)} p$ reaction was studied by the COMPASS collaboration at beam energies of 191 GeV and the narrow interval of target-recoil 4-momentum transfer squared of 0.1 GeV^2 $< -t <$1.0 GeV^2. For the $\pi\eta^{(\prime)}$ CMS energies (invariant masses) above the resonance region, *i.e.* $M_{\pi\eta} \gtrsim$ 2 GeV, this process is dominated by the double Regge exchanges. Two types of diagrams represent these exchanges.

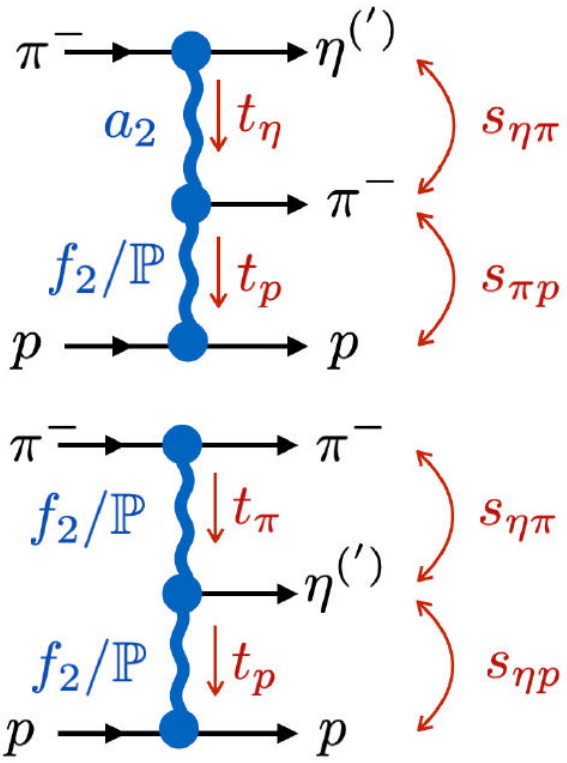

FIGURE 1. Fast-η (top) and fast-π (bottom) amplitudes.

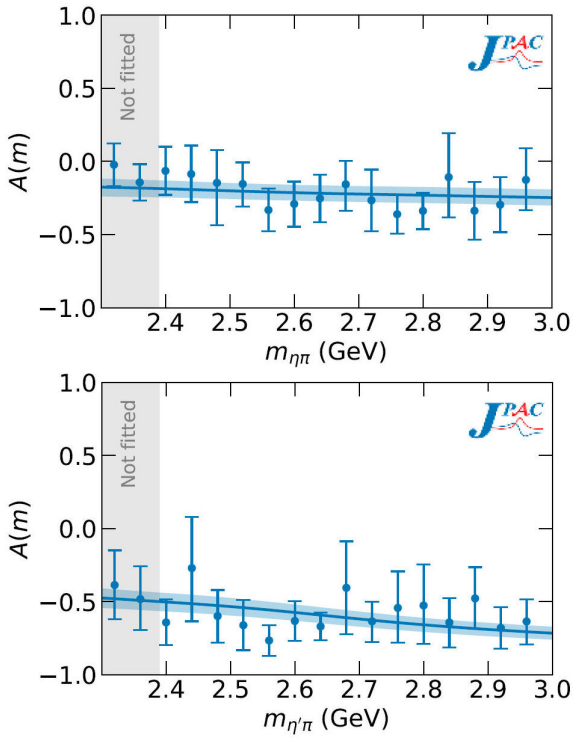

FIGURE 2. Forward-backward intensity asymmetry for $\eta\pi$ (upper plot) and $\eta'\pi$ (lower plot) from Ref. [6].

For type I diagrams (a.k.a. fast η diagrams) a_2 trajectory can be exchanged in the upper line and either f_2 or pomeron trajectories in the lower line. For type II diagrams (a.k.a. fast π diagrams) either f_2 or pomeron trajectories can be exchanged in both upper and lower lines. Both types of diagrams are shown in Fig. 1.

Type I and type II diagrams altogether represent 6 amplitudes whose relative strengths are unknown due to difficult to evaluate reggeon-reggeon-meson couplings. Therefore, in what follows we treat the amplitude strengths as fit parameters. The general form of individual exchange amplitudes is defined in Eq. (1), where $s_1 = s_{\pi\eta}$ and $s_2 = s_{\pi p}$ for type I amplitudes and $s_1 = s_{\pi\eta}$ and $s_2 = s_{\eta p}$ for type II amplitudes. The t variables in Regge trajectories are replaced accordingly. The ξ_1, ξ_2, ξ_{12} and ξ_{21} factors are related to signatures of individual trajectories. These signatures are all kept +1 since the J^{PC} quantum numbers are 2^{++} for all considered trajectories.

$$T = -K\Gamma(1-\alpha_1)\Gamma(1-\alpha_2)\Big[(\alpha' s)^{\alpha_1-1}(\alpha' s_2)^{\alpha_2-\alpha_1} \times \xi_1\xi_{21}\hat{V}_1 + (\alpha' s)^{\alpha_2-1}(\alpha' s_1)^{\alpha_1-\alpha_2}\xi_2\xi_{12}\hat{V}_2\Big]. \quad (1)$$

Definitions of other amplitude components like the kinematical factor K and the V_1 and V_2 terms can be found in Ref. [5].

Before we move on to discuss our fit results it is worth mentioning one technical aspect of the fitting procedure. Even though the COMPASS data were given in terms of the partial wave intensities and phases relative to the $L = 2$, $M = 1$ partial wave, it was impossible to fit the model directly to these data. The reason is that the experimental partial waves which were truncated at a $L = 6$ were normalized so that the integrated angular distribution was equal to the total experimental yield. Therefore, the model could be compared with the data only at the level of the full (rather than partial wave projected) amplitudes. Details of the fit procedure as well as parameter values and their uncertainty estimations can be found in Ref. [6]. Having established the model parameter values we were able to predict the angular distributions in polar and azimutal angles for both $\pi\eta$ and $\pi\eta'$ channels as well as the invariant mass dependent intensities. However, the quantity which best illustrates the $\pi\eta^{(\prime)}$ production asymmetry is the forward backward asymmetry defined by Eq. (2a). Even though this quantity was not directly presented in the COMPASS analysis we were able to evaluate it along with statistical uncertainty using experimental partial waves and the statistical bootstrap procedure.

$$A(m) \equiv \frac{F(m) - B(m)}{F(m) + B(m)}, \quad (2a)$$

$$F(m) \equiv \int_0^1 \cos\theta\, I_\theta(m, \cos\theta)\,, \quad (2b)$$

$$B(m) \equiv \int_{-1}^0 \cos\theta\, I_\theta(m, \cos\theta)\,. \quad (2c)$$

In Fig. 2 we compare forward-backward asymmetries obtained from the model with those reproduced from the COMPASS data, for both $\pi\eta$ and $\pi\eta'$ channels. The two lowest invariant mass data points shown in the gray area of both plots of Fig. 2 were not fitted in the analysis. This was because the model discussed here applies to the region of large $\pi\eta$ invariant masses governed by the Regge dynamics. The two bins in question were, however, affected by the resonances. Still, we show the asymmetry in the intermediate region to highlight the good matching of the Regge and resonance regimes. Finally, it is worth mentioning that as expected from the raw (not acceptance corrected) polar angle distributions from COMPASS analysis (see Fig. 2 in [3]), the asymmetry effect is much stronger for the $\pi\eta'$ channel, which is in line with model predictions.

3. $\pi^+\pi^-$ photoproduction

Even though the $\gamma p \to \pi^+\pi^- p$ reaction has been studied for over 50 years a comprehensive description of the $\pi^+\pi^-$ photoproduction in low partial waves is still missing. There are several reasons for that. First of all, the data sets available so far were not sufficient to perform the partial wave analysis beyond the dominant $P-$wave, with the $\rho(770)$ as a most pronounced state. Secondly, for the photon energies of a few GeV the dynamics of the process is inherently complex with the direct resonance production (modelled by the Reggeon exchange) accompanied by target excitation effects. The target excitation effects can in turn lead to secondary rescattering in the meson channel, which is known as the Deck process and is diagramatically shown in Fig. 3.

The important feature of the Deck process is that the $\pi^+\pi^-$ production is mainly driven by the one pion exchange. This is because the pion exchange is related to the amplitude singularity which is closest to the physical region of $\pi^+\pi^-$ production. This way we arrive at the picture where the $\pi^+\pi^-$ pair arises due to two complementary mechanisms: the direct resonance production with subsequent decay to $\pi^+\pi^-$ channel and the photon dissociation to $\pi^+\pi^-$ pair with one of the pions brought on shell through scattering off the target (with possible $\pi\pi$ re-scattering). In the first mechanism the pion source is point-like whereas in the second one it is rather diffuse due to the long range nature of the pion exchange. As was shown in Ref. [7] the general structure of the amplitude for such process is

$$T_{\pi\pi} = M_{\text{compact}} \sin\delta_{\pi\pi} e^{i\delta_{\pi\pi}} + M_{\text{diffuse}} \cos\delta_{\pi\pi} e^{i\delta_{\pi\pi}}\,, \quad (3)$$

where for simplicity we have omitted the kinematical and polarisation variables. In the exploratory study presented in [8] we have used the simplified form of the M_{compact} amplitude which captured just the fact that it should be structure-less in the $\pi\pi$ energy while neglecting its spin structure. This was justified by the fact that the amplitudes were intended to describe unpolarized mass distributions obtained by CLAS [4] where the spin averaged formalism was sufficient. Thus, the simplest structure-less parametrization of the short range term has the linear form

$$M_{\text{compact}} = A + B s_{\pi\pi}, \quad (4)$$

with the A and B parameters fitted independently for each partial wave (see [8] for details).

To parameterize the Deck amplitudes we employed precise information on the πp scattering encoded in SAID partial wave amplitudes [9]. The general form of the gauge invariant Deck helicity amplitude reads

$$M_{\lambda_2\lambda\lambda_1} = -e\Bigg[\left(\frac{\epsilon_\lambda\cdot k_2}{q\cdot k_2} - \frac{\epsilon_\lambda\cdot(p_1+p_2)}{q\cdot(p_1+p_2)}\right) T^+_{\lambda_1\lambda_2} - \left(\frac{\epsilon_\lambda\cdot k_1}{q\cdot k_1} - \frac{\epsilon_\lambda\cdot(p_1+p_2)}{q\cdot(p_1+p_2)}\right) T^-_{\lambda_1\lambda_2}\Bigg] \quad (5)$$

where q, p_1, p_2, k_1 and k_2 are respectively the 4-momenta of the photon, target proton, recoil proton, positive and negative pions, ϵ_λ is the photon polarisation 4-vector for photon helicity λ and $T^+_{\lambda_1\lambda_2}$, $T^-_{\lambda_1\lambda_2}$ are helicity amplitudes of pion-proton elastic scattering for positive and negative pion, respectively. These amplitudes were expressed in terms of SAID partial waves. It is worth mentioning that the Deck component of the full amplitude which relies on the SAID parametrization is essentially parameter free. To obtain the partial wave mass distributions in the $\pi^+\pi^-$ system, the full amplitude consisting of the direct production and Deck terms was partial wave projected according to Eq. (6)

$$T^{lm} = \int d\Omega\; Y^*_{lm}(\Omega)\;(M_{\text{compact}} + M_{\text{diffuse}}), \quad (6)$$

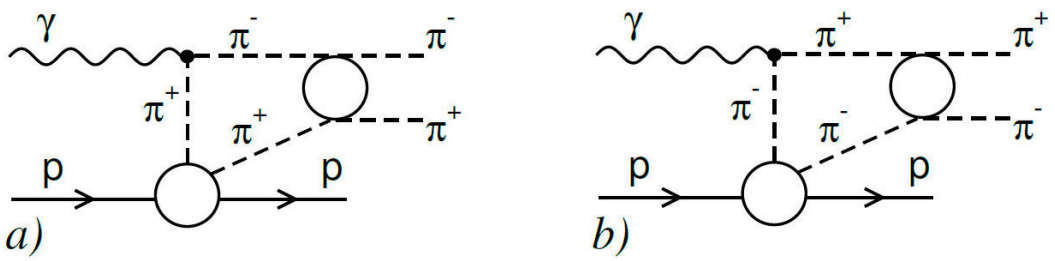

FIGURE 3. Diagrams for the pion photoproduction (Deck mechanism), where pions are subject to final state interactions.

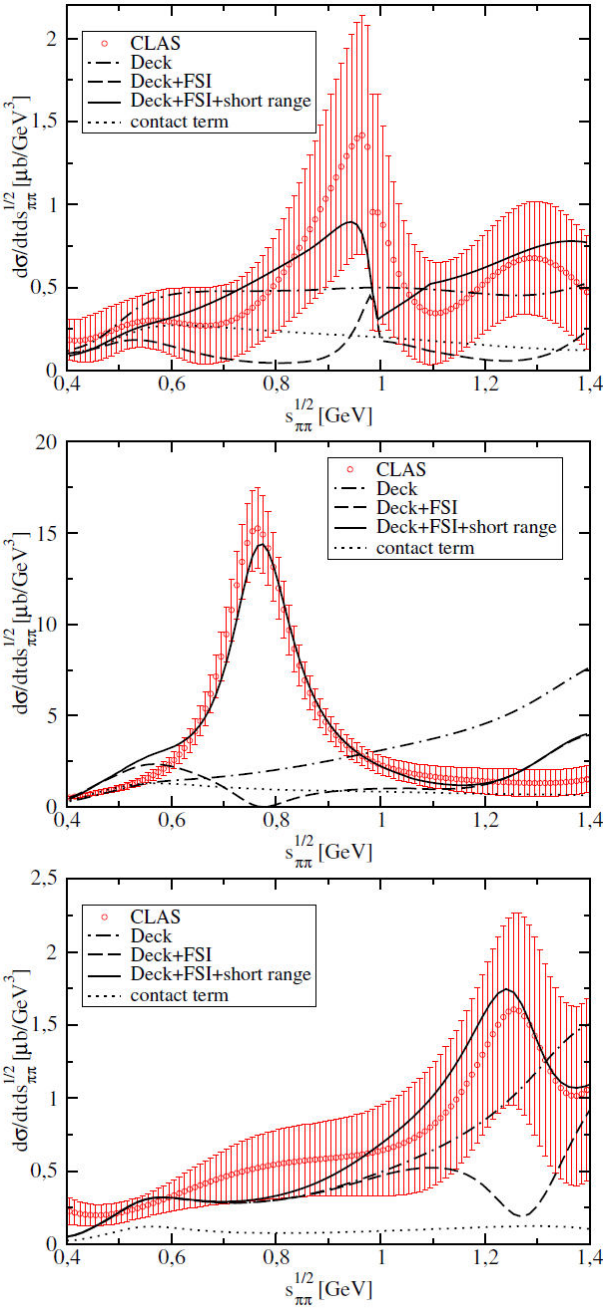

FIGURE 4. $S-$, $P-$ and $D-$wave invariant mass distributions for the model with direct resonance production and Deck background.

where helicity indices were again omitted for simplicity. To describe the final state $\pi\pi$ re-scattering in the Deck amplitudes and the resonance line shape in the direct resonance production we have used the $\pi\pi$ phase shifts developed in [10]. The partial wave projected amplitude from Eq. (3) was then used to compute the double differential partial wave mass distributions according to the formula

$$\frac{d^2\sigma}{d|t|\,d\sqrt{s_{\pi\pi}}} = \frac{1}{64(2\pi)^4}\frac{|\mathbf{k}|}{(s-m^2)^2}\sum_{lm}\sum_{\lambda_2\lambda\lambda_1}|T^{lm}_{\pi\pi}|^2\,. \quad (7)$$

By fitting just two parameters A and B for each partial wave, we were able to describe the mass distributions for the $S-$, $P-$ and $D-$waves as shown in Fig. 3. As expected, the distributions are dominated by resonance lines of $f_0(980)$, $\rho(770)$ and $f_2(1270)$, respectively.

An important observation from partial wave mass distributions in Fig. 4 is that for the the $P-$ and $D-$ waves the Deck+FSI contribution is strongly suppressed in the resonance region so that the process is dominated by the direct resonance production. This is compatible with the commonly accepted notion that the $\rho(770)$ and $f_2(1270)$ are conventional $q\bar{q}$ states. On the other hand, the Deck contribution is quite substantial in the $S-$wave with the Deck+FSI term being decisive in description of the resonance shape near 1 GeV. This in turn may imply that the $f_0(980)$ state contains a sizable molecular or tetraquark component.

4. Conclusions and outlook

We have discussed the models for the $\pi\eta^{(\prime)}$ and $\pi^+\pi^-$ production at high energies. The double Regge exchange model with 2^{++} Regge trajectories successfully describes the angular and mass dependent intensities for $\pi\eta^{(\prime)}$ energies above the resonance region. The model also accounts for the observed forward-backward asymmetry in the $\pi\eta^{(\prime)}$ polar angle distributions as well as for the fact that the phenomenon is stronger for the $\pi\eta'$ channel. This hints to the role of gluonic degrees of freedom in the η' production which is in line whith it being mostly an SU(3) singlet.

We have also shown that the combination of the direct resonance production (short range/compact source) and the Deck mechanism (long range/diffuse source) is able to provide a satisfactory description of the $\pi^+\pi^-$ photoproduction in the resonance region. The relative contributions of the compact source and diffuse source mechanisms for the $P-$, $D-$ and $S-$waves are in line with the $q\bar{q}$ nature of the former and possibly molecular or tetraquark nature of the latter.

Quite remarkably, the two models in their current version are designed to work in complementary meson-meson energy regions. The double Regge exchange model describes the $\pi\eta^{(\prime)}$ system production for invariant masses above 2 GeV while the $\pi^+\pi^-$ photoproduction model captures mainly the the resonance dynamics of the $\pi^+\pi^-$ system. Finite energy sum rules (FESR) make it possible to match the amplitudes in these two energy regions. Works to provide the unified description of the di-meson systems both in the resonance and Regge exchange regions are currently underway in the JPAC collaboration.

1. A. P. Szczepaniak and M. Swat, *Role of photoproduction in exotic meson searches*, Phys. Lett. B **516** (2001) 72 https://doi.org/10.1016/S0370-2693(01)00905-4.
2. B. Ketzer, B. Grube and D. Ryabchikov, *Light-Meson Spectroscopy with COMPASS*, Prog. Part. Nucl. Phys. **113** (2020) 103755 https://doi.org/10.1016/j.ppnp.2020.103755.
3. C. Adolph *et al.* [COMPASS], *Odd and even partial waves of $\eta\pi^-$ and $\eta'\pi^-$ in $\pi^- p \to \eta^{(\prime)}\pi^- p$ at 191 GeV/c*, Phys. Lett. B **740** (2015) 303 [erratum: Phys. Lett. B **811**, 135913 (2020)] https://doi.org/10.1016/j.physletb.2014.11.058.
4. M. Battaglieri *et al.* [CLAS], *Photoproduction of pi+ pi- meson pairs on the proton*, Phys. Rev. D **80** (2009) 072005 https://doi.org/10.1103/PhysRevD.80.072005.
5. R. C. Brower, C. E. DeTar and J. H. Weis, *Regge Theory for Multiparticle Amplitudes*, Phys. Rept. **14** (1974) 257 https://doi.org/10.1016/0370-1573(74)90012-X.
6. L. Bibrzycki *et al.* [JPAC], *," $\pi^- p \to \eta^{(\prime)}\pi^- p$ in the double-Regge region* Eur. Phys. J. C **81** (2021) 647 [erratum: Eur. Phys. J. C **81**, no.10 (2021) 915] https://doi.org/10.1140/epjc/s10052-021-09594-8.
7. I. J. R. Aitchison and M. G. Bowler,

   Rescattering Effects in the Deck Model, J. Phys. G **3** (1977) 1503 https://doi.org/10.1088/0305-4616/3/11/007.
8. Ł. Bibrzycki, P. Bydžovský, R. Kamiński and A. P. Szczepaniak, *Meson resonances in forward-angle $\pi^+\pi^-$ photoproduction*, Phys. Lett. B **789** (2019) 287 https://doi.org/10.1016/j.physletb.2018.12.045.
9. SAID, R.L. Workman, R.A. Arndt, W.J. Briscoe, M.W. Paris, I.I. Strakovsky, Phys. Rev. C **86** (2012) 035202 https://doi.org/10.1103/PhysRevC.86.035202; http://gwdac.phys.gwu.edu/.
10. P. Bydžovský, R. Kamiński and V. Nazari, *Dispersive analysis of the S-, P-, D-, and F-wave $\pi\pi$ amplitudes* Phys. Rev. D **94** (2016) 116013 https://doi.org/10.1103/PhysRevD.94.116013.